A study on the behavior of underwater shock waves generated in a water container and its application to magnetic refrigeration material

Young Kook Kim[1], Shigeru Itoh[2]
[1]Graduate School of Science and Technology, Kumamoto University
2-39-1 Kurokami, Kumamoto City, Kumamoto, 860-8555, Japan
E-mail: kim@shock.smrc.kumamoto-u.ac.jp
[2]Shock Wave and Condensed Matter Research Center,
Kumamoto University 2-39-1 Kurokami,
Kumamoto City, Kumamoto, 860-8555, Japan
E-mail: itoh@mech.kumamoto-u.ac.jp

ABSTRACT
Most of composite materials are made by sintering method. In this research, in order to make composite material for magnetic refrigeration, we carried out several experiments for the powder consolidation using the shock compaction method and numerical analysis for the behavior of underwater shock wave. The shock compaction method is to consolidate metal powder using underwater shock wave including an ultra-high pressure and high velocity generated by detonation of explosive. Generally, the magnitude of peak pressure and the pressure distribution of underwater shock wave depend on the inner shape of water container which is one of the parts of high pressure generating device. In this study, we have investigated several water containers using numerical analysis and observation experiments. Therefore, underwater shock wave is affected by the reflected wave generated from the wall of water container and the magnitude of reflected wave depends on the inner angle θ of water container. The pressure and velocity of reflected wave is gradually increased with increasing inner angle θ of water container.

Keywords: Shock compaction Method; Underwater shock wave; Powder consolidation

1. INTRODUCTION

Recently, interest in magnetic material which exhibits a ferromagnetic property near room temperature has been increasing in order to realize the magnetic refrigeration. Most of magnetic materials are made by the sintering methods.[1,2] In this study, a shock compaction method which uses an underwater shock wave generated by the detonation of explosive is used. The shock compaction method has an advantage such as the grain size of metal powder can be minimized because of ultra-high pressure and high velocity. This is a good thing in terms of magnetic property.[3-5] Therefore, in order to consolidate the magnetic metal powder, we have carried out the consolidating experiments using ultra-high pressure

generation devices. The ultra-high pressure generation device is composed of several parts; electric detonator, explosive lens, explosives, explosive container and water container. The most important part is the water container, because the pressure distribution and pressure magnitude of underwater shock wave absolutely depend on the inner shape of water container. Accordingly, the purpose of this research is to propose an optimal model of water container designed by numerical analysis.

2. ULTRA-HIGH PRESSURE GENERATION DEVICE

The ultra-high pressure generation device used in this study is shown in figure 1. The main parts are composed of an explosive container, water container and powder container. Explosive, water and magnetic powder are set in each container. The main explosive is SEP which made of PETN(65wt.%) and paraffin (35wt.%), detonation velocity of 6970m/s and C-J pressure of 15.9GPa produced by Asahi chemical Co. Ltd, Japan.[6]

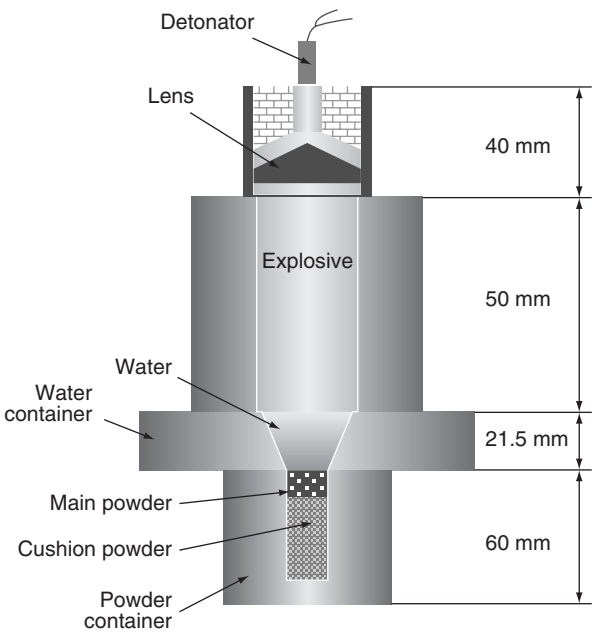

Figure 1 The schematic of the ultra-high pressure generation device

The explosive lens that is composed of SEP and HABW (detonation velocity; 4500m/s and density; 2200kg/m^3 produced by Asahi-Kasei Chemicals Corp) is set on the top of the main explosive to make a planar wave. Explosion is started from detonator and the detonation wave generated by explosive propagated into the water container which creates underwater shock wave of high pressure. High velocity occurs in the water container.

3. NUMERICAL ANALYSIS FOR THE WATER CONTAINER

In order to make a good consolidated bulk material, a planar wave on the top surface of powder is necessary. The pressure distribution and pressure magnitude of underwater shock wave depend on the inner shape of the water container. Therefore a series of phenomenon for the explosion and propagation of underwater shock wave is evaluated by means of LS-DYNA 3D (commercial program based on the explicit finite element code). The numerical simulation model is shown in figure 2. The simulation model is modeled as quarter of circle.

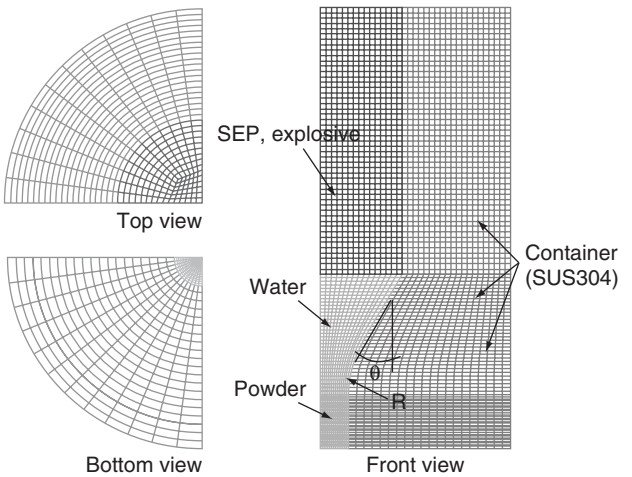

Figure 2 Numerical simulation model

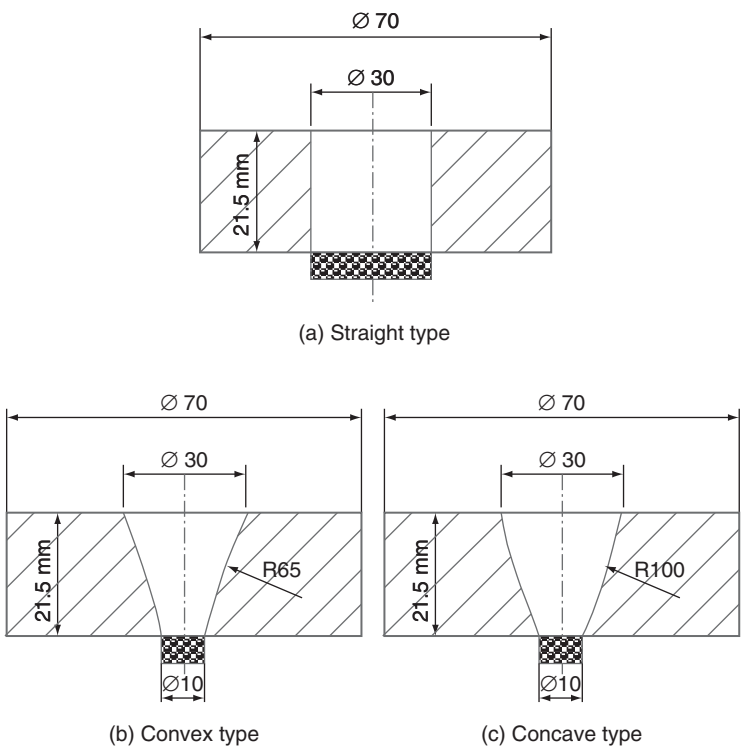

Figure 3 Schematic of water container models

In boundary condition, initial velocity is 1711m/s as particle velocity of explosive and we applied the constrained condition for the x, y, and z axis so that translational and rotational motions can not happen when explosion is occurring. The materials on the both sides of the surface are distinguished as master and slave, respectively. In the selection of the salve and master part, the material with greater density is chosen as the master. A null material model

for water is applied and an elastic-plastic hydrodynamic material model for each container is used. In the case of powder material, it's modeled as a part of null material because we just need the distribution and magnitude of pressure of underwater shock wave impinged on the top surface of powder. The C-J detonation process of explosive is modeled using 'C-J volume burn' method. Water container models, straight type, convex type and concave type, for numerical simulation are shown in figure 3.

3.1. JONES-WILKINS-LEE EQUATION OF STATE

JWL equation of state is applied for the explosive. JWL coefficients and the main C-J characteristic values are given in Table 1. JWL equation of state is as follows; [7]

$$P_{JWL} = A\left[1-\frac{\omega}{VR_1}\right]\exp(-R_1V)+B\left[1-\frac{\omega}{VR_2}\right]\exp(-R_2V)+\frac{\omega e}{V} \tag{1}$$

A, B, C, R_1, R_2 and ω are the constants for a given explosive. P_{JWL} is pressure, e is the specific internal energy, and V is ρ_0/ρ_g (Initial density of an explosive divided by the density of detonation gas).

Table 1 JWL coefficients and C-J values of SEP

A(Gpa)	B(Gpa)	R1	R2	Ω
364	2.31	4.3	1.00	0.28

3.2. C-J VOLUME BURN & MIE-GRUNEISEN EQUATION OF STATE

In order to resolve the reaction occurred in high explosive, 'C-J volume burn' model is applied.[23] When the volume of the cell of the original explosive in the calculation becomes equal to the volume of the detonation products at Chapman-Jouguet (C-J) state, the solid-phase explosive is assumed to be completely decomposed into the gaseous products. If V_0 express the initial volume of explosive, V_{CJ} is the volume of the detonation products at the C-J state. The reaction rate of the explosive is simply expressed as follows;

$$W = 1-\frac{V_0-V}{V_0-V_{CJ}}\ ,\ V_0 \le V \le V_{CJ} \tag{2}$$

$$P = (1-W)P_{JWL} \tag{3}$$

Decomposition rate W of the explosive has values from 0 to 1. P_{JWL} is the pressure of detonation products of the completely reacted explosive and can be obtained from JWL equation. P is assumed to be equal to that of the detonation products of the partly reacted explosive over the whole cell. Metal materials concerned with numerical simulation are applied to be elastic-plastic-hydrodynamic material comply with the von Mises yield criterion for the distinction of elastic and plastic phases. Accordingly, Mie-Gruneisen equation of state is applied and it's given as follows;

$$P = \frac{\rho_0 C_0^2 \eta}{(1-s\eta)^2}\left[1-\frac{\Gamma_0\eta}{2}\right]+\Gamma_0\rho_0 e \tag{4}$$

η: 1 – ρ(*Initial density of the medium*) / ρ(Density of the medium)
P: Pressure
e: Specific int*ernal* energy
C, s: Cons tant *of material*
Γ: Grüeisen coefficient

The parameters of water and SUS304 stainless steel for container are shown in table 2.

Table 2 Mie-Gruneisen parameter of water and SUS304

	ρ_0(kg/m^3)	Co(m/s)	s	Γ_0
Water	1000	1489	1.79	1.65
SUS304	7900	4570	1.49	2.17

3.3. NUMERICAL SIMULATION RESULTS

We have analyzed several water containers to obtain a good pressure distribution and proper pressure magnitude of underwater shock wave impinging on the top surface of powder. The underwater shock wave propagation on the top surface of the powder for each water container is shown in figure 4. When a detonation wave occurred due to the explosion by explosive enters the water, the underwater shock wave is created and then a reflected wave occurs from the wall of the container and converges at the middle point, creating ultra high pressure.

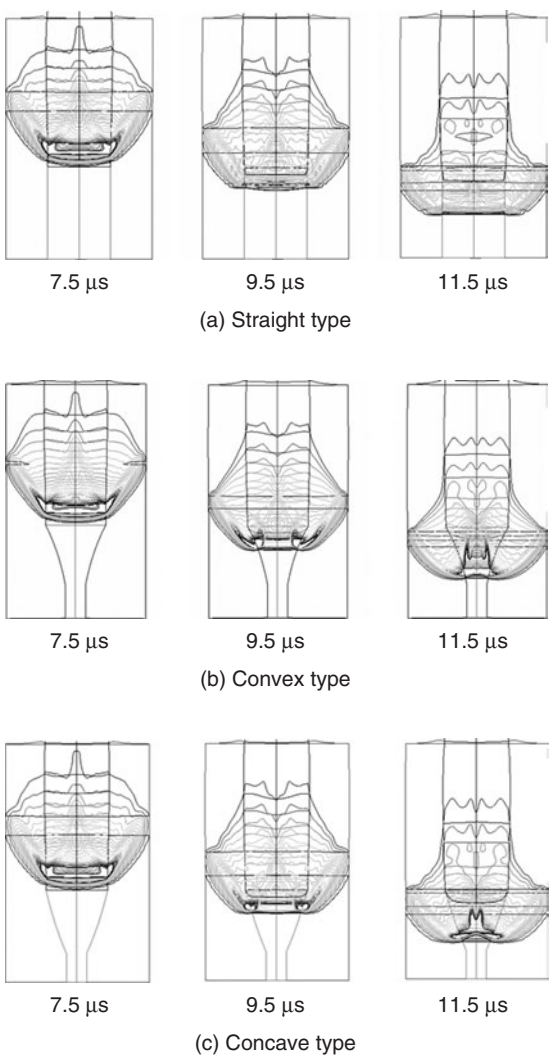

Figure 4 The propagation phenomenon of underwater shock wave for each water container

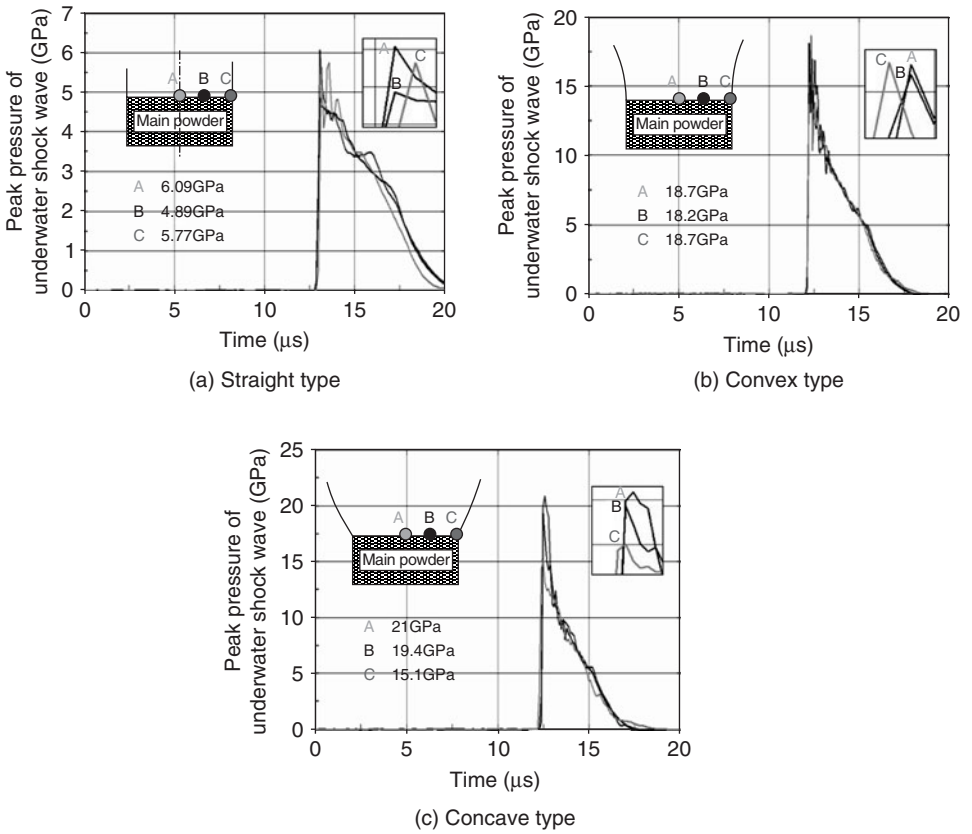

Figure 5 Peak pressure of underwater shock wave impinged on the top surface of powder for each water container

The peak pressure profiles of underwater shock wave impinged on the top surface of powder obtained at the central position (A), middle position (B), near wall position (C) are shown in figure 5. In the straight type case, the reflected wave is small compared to the detonation wave, and the duration time of pressure acting on the top surface of the powder is longer than other models. Whereas, the pressure magnitude is lower. In case of convex type, the distribution of peak pressures for each position is better than that of other models, and we found that it has the proper pressure magnitude to consolidate the magnetic powder. In the case of concave type, it has a large volume in comparison with convex type. Although the inner angle θ of water container is small, the pressure magnitude is higher than that of convex type. Accordingly, it can be confirmed that the pressure magnitude of underwater shock wave is related to the shape of water container. Figure 6 shows pressure distribution diagrams for each water container. The detonation of the explosive generates a shock wave in the water. This underwater shock wave is modified by the shape of the water container. A Mach reflection occurs from the wall of the container and converges at the center line, creating ultra high pressure.[8-9] The reflected wave continues through the center line decreasing from ultra high pressure. Finally, the reflected wave and underwater shock wave are united and impinge on the top surface of the powder at about t=12μs. The pressure magnitude of reflected wave at the central portion of the water container is increased with

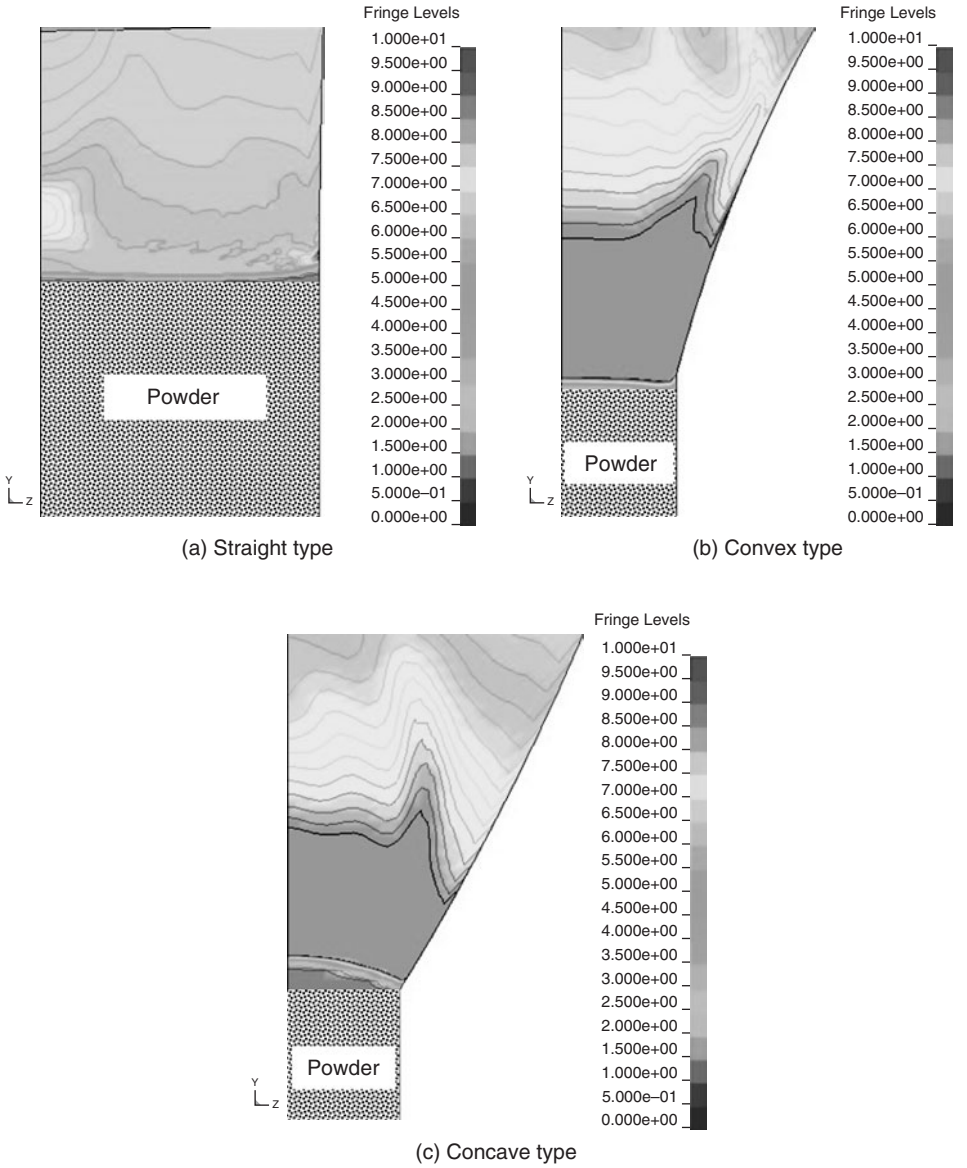

Figure 6 Pressure distribution diagrams of underwater shock wave impinged on the top surface of powder for each water container

increasing inner angle θ of water container. The underwater shock wave is affected by the reflected wave. The straight type has a poor distribution with 6.09GPa at central position (A), 4.89GPa at middle position (B) and 5.77GPa at the wall (C). In the case of convex type, pressure distribution of underwater shock wave is better than that of the others with 18.7GPa at central position (A), 18.2GPa at the middle position (B) and 18.7GPa at the wall(C). In concave type case, pressure magnitude is higher than others; however the pressure distribution of underwater shock wave is not good. It has 21GPa at central position (A),

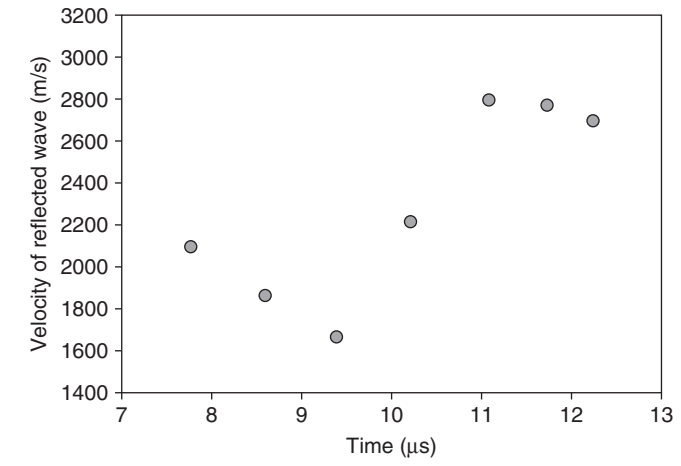

(a) Velocity change of reflected wave at the central position of water container

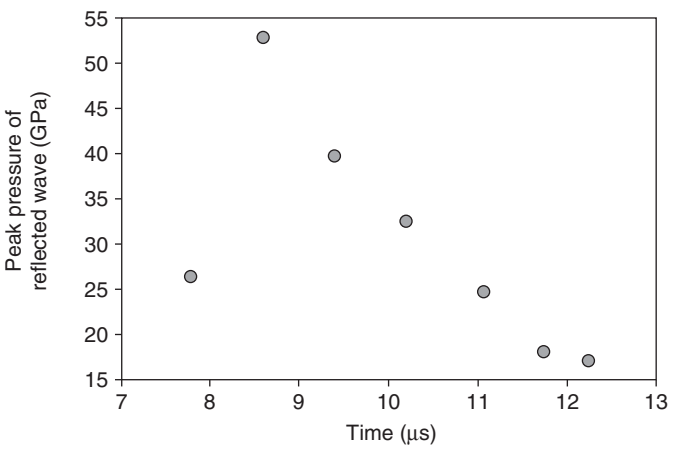

(b) Pressure magnitude of reflected wave at the central position of water container

Figure 7 Pressure magnitude and velocity change of reflected wave at the central position along with axis direction in the water container in the convex type

19.4GPa at the middle position (B) and 15.1GPa at the wall (C). Figure 7 is represented the pressure magnitude and velocity change at the central position along with axis direction in the water container in the convex type. It's considered that the gathering of reflected wave in the middle position of water container occurred between 8 and 9 μs. At 9 μs, the peak pressure of reflected wave is decreased whereas, the velocity of reflected wave is gradually increased after 10 μs. We confirmed that the velocity of underwater shock wave is not affected by reflected wave until the moment the reflected wave is converged in the middle position.

3.4. OBSERVATION EXPERIMENT OF UNDERWATER SHOCK WAVE

The observation experiment is carried out to observe the behavior of underwater shock wave and the reflected wave in the water to verify numerical analysis results. The test device is a planar symmetric setup to allow viewing the shock wave.

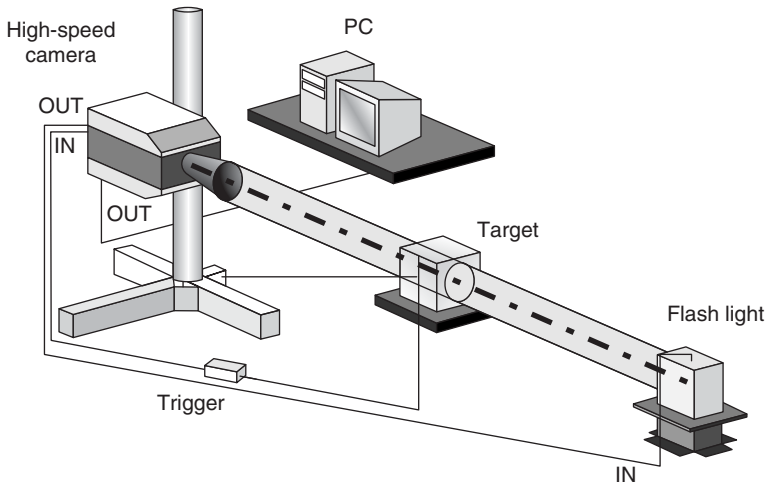

Figure 8 Schematic of observation measurement system

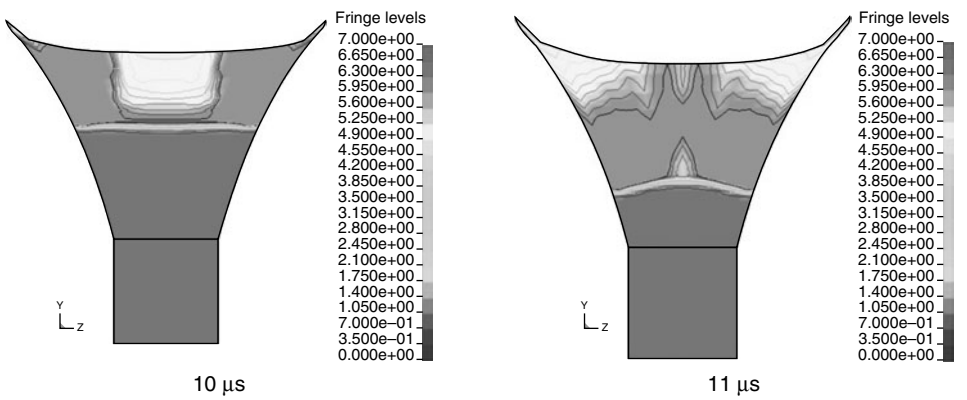

(a) Pressure diagram of underwater shock wave

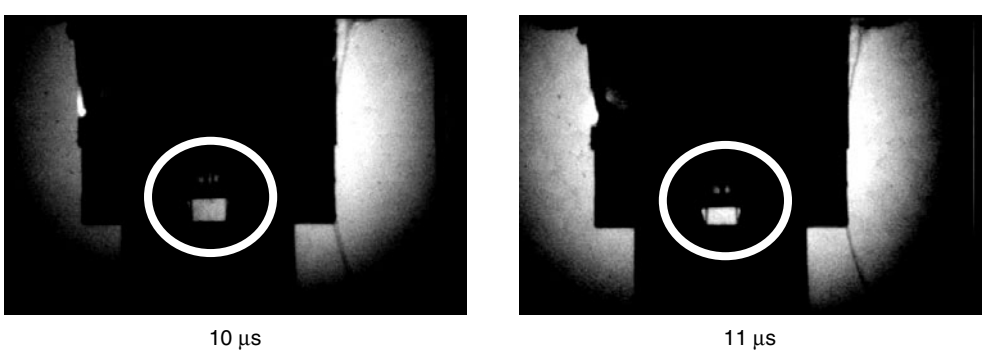

(b) Framing photographs of underwater shock wave

Figure 9 Pressure diagram and framing photograph for the underwater shock wave in the case of convex type

The test device is set in the explosion chamber and a high-speed camera system, IMACON 468(Hadland Photonics), is equipped with Xenon Flash for observation. The start of the photography is controlled by ionization wire probes inserting into the test device which can be connected with trigger. The schematic of observation experiment system is shown in figure 8.[10] Figure 9 shows the comparison between result of numerical analysis and framing photograph of underwater shock wave in the case of convex type. Based on validation of simulation by the experiment of 2D type, the 3D model should also be sufficient to simulate the shock wave in the axisymmetric water container.

3.5. MEAN PEAK PRESSURE MEASUREMENT

In order to check the peak pressure of underwater shock wave, we carried out the pressure measurement experiment using manganin gauge as designed by Mashimo et al. [11] Figure 10 shows the mean peak pressure of underwater shock wave obtained from the experiment and numerical analysis. The mean peak pressure for the experiment and numerical analysis is 16.8GPa and 17.9GPa, respectively. The difference is similar to the measurement error of 1GPa, confirming the ability of the numerical analysis to predict the pressure in the water container.

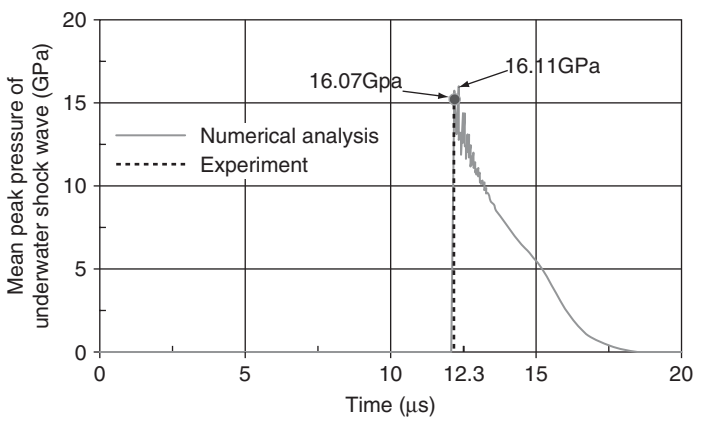

Figure 10 Comparison between mean peak pressure of numerical analysis and real experiment for the underwater shock wave impinged on the top surface of powder

4. APPLICATION TO CONSOLIDATING EXPERIMENT

We have carried out the experiment for the metal powder consolidation based on the results of numerical analysis. The metal powders used in this study are $MnSi_4Fe_3$ and $La Co_{0.7}Si_{1.1}Fe_{11.2.}$ Figure 11 shows the cross sectional photographs of the consolidated bulk materials. We found that the consolidation using underwater shock wave is good and also confirmed that the grain size is similar to the starting powder.

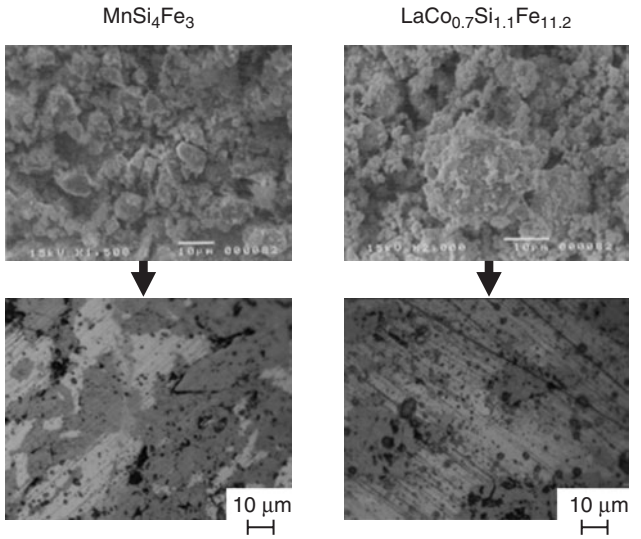

Figure 11 Consolidated bulk materials using shock compaction method

5. CONCLUSION

We have analyzed several water containers, one of the parts of the ultra-high pressure generation device, using numerical analysis and verified it through the experiment. We found that the velocity and pressure of underwater shock wave is affected by the reflected wave generated from wall and the magnitude of reflected wave is increased with increasing inner angle θ of water container. Also, the pressure magnitude of underwater shock wave is related to the shape of the water container. We confirmed that the grain size of the initial powder is maintained in the consolidated bulk material. In case of convex type, the distribution of peak pressures for each position is better than that of other models. Lastly, the experimental and numerical mean peak pressure is 16.11GPa and 16.07GPa, respectively.

REFERENCES

[1] Percharsky, V.K. & Gschneidner, K.A.Jr, Giant magnetocaloric effect in Gd5(Si_2G_2), Phys. Rev. Lett. 78, (1997) 4494–4497.

[2] O.Tegus, E. Bruck, K.H.J Buschow & F. R. de Boer, Transition-metal-based magnetic refrigerants for room-temperature applications, NATURE. 415, (2002) 10 January.

[3] S. Ando, Y. Mine, K. Takashima, S. Itoh, H. Tonda, Explosive compaction of Nd-Fe-B powder, Journal of materials processing technology, 85, (1999)142–147.

[4] Z.Q. Jin, N.N. Thadhani, M. McGill, J. Li, Y. Ding, Z.L. Wang, H. Zeng, M. Chen, S.F. Cheng, J. P. Liu, Grain size dependence of magnetic properties in shock synthesized bulk $Pr_2Fe_{14}B/\alpha$-Fe nanocomposites, Journal of Apply Physics. 96(6), (2004) 3452–3457.

[5] Z.Q. Jin, K.H. Chen, J. Li, H. Zeng, S.F. Cheng, J. P. Liu, Z.L. Wang, N.N. Thadhani, Shock compression response of magnetic nanocomposite powders, Acta Materialia 52, (2004) 2147–2154.

[6] S. Itoh, T. Hamada, K. Murata, High Pressure Generation Using Underwater Explosion of a spiral Explosive in a conical Vessel, Emerging Technologies in Fluids, Structures, and Fluid/Structure Interactions, ASME 2002, 2, (2002) 197–202.

[7] Lee, E.L., Hornig, H.C. and Kury, J.W. " Adiabatic Expansion of High Exposive Detonation Products" Lawrence Livemore National Laboratory report UCRL-50422(1968).

[8] Y. Nadamitsu, Z.Y. Liu, M. Fujita, S. Itoh., Von Neumann reflection of underwater shock wave, Journal of materials processing technology, Vol 85, (1999) 48–51.

[9] Y. Matsui and S. Itoh, Evauluation of Ultra-High Pressure Generating Device by Numerical Simulation, ASME/JSME Pressure Vessels and Piping Conference, PVP-Vol 485–2, (2004).

[10] A. Kira, M. Fujita, S. Itoh, Underwater explosion of sperical explosives, Journal of materials processing technology, Vol 85, (1999) 64–68.

[11] Akira Nakamura, Tsutomu Mashimo, Calibration Experiments of a Thin Manganin Gauge for Shock-Wave measurement in Solids: Measurements of Shock-Stress History in Alumina, Journal of Apply Physics. 32, (1993) 4785–4790.

ACKNOWLEDGEMENT

This work was supported by 21st Century COE program. We would like to express our thanks for financial assistance in order to conduct this research.